

Galectin-1-mediated high NCAPG expression correlates with poor prognosis in gastric cancer

Tingrui Zheng^{1,*}, Tao Qian^{2,*}, Haihua Zhou¹, Zhiyi Cheng¹, Guiyuan Liu¹, Chuanjiang Huang¹, Rongrong Dou³, Fuxing Liu³, Xiaolan You¹

¹Department of Gastrointestinal Surgery, The Affiliated Taizhou People's Hospital of Nanjing Medical University, Taizhou 225300, Jiangsu, China

²Department of Anesthesiology, The Affiliated Taizhou People's Hospital of Nanjing Medical University, Taizhou 225300, Jiangsu, China

³Department of the Pathology, The Affiliated Taizhou People's Hospital of Nanjing Medical University, Taizhou 225300, Jiangsu, China

*Equal contribution

Correspondence to: Xiaolan You; email: 006586@yzu.edu.cn

Keywords: gastric cancer, Galectin-1, NCAPG, prognosis, metastasis

Received: March 27, 2023

Accepted: May 24, 2023

Published: June 16, 2023

Copyright: © 2023 Zheng et al. This is an open access article distributed under the terms of the [Creative Commons Attribution License](https://creativecommons.org/licenses/by/3.0/) (CC BY 3.0), which permits unrestricted use, distribution, and reproduction in any medium, provided the original author and source are credited.

ABSTRACT

Galectin-1 (Gal1) and non-SMC condensin I complex, subunit G (NCAPG) are associated with metastasis in several malignant tumors. However, their precise roles in gastric cancer (GC) remain uncertain. This study explored the clinical significance and relationship of Gal1 and NCAPG in GC. Gal1 and NCAPG expressions were significantly up-regulated in GC compared to adjacent non-cancerous tissues by immunohistochemistry (IHC) and Western blotting. Besides, methods including stable transfection, quantitative real-time reverse transcription PCR, Western blotting, Matrigel invasion and wound-healing assays *in vitro*, were also conducted. IHC scores for Gal1 and NCAPG had a positive correlation in GC tissues. High Gal1 or NCAPG expression significantly correlated with poor prognosis in GC, and Gal1 combined with NCAPG had a synergetic effect on the prediction of GC prognosis. Gal1 overexpression *in vitro* enhanced NCAPG expression, cell migration, and invasion in SGC-7901 and HGC-27 cells. Simultaneous Gal1 overexpression and NCAPG knockdown in GC cells partly rescued the migrative and invasive abilities. Thus, Gal1 promoted GC invasion through increased NCAPG expression. The present study demonstrated the prognostic significance of the combination of Gal1 and NCAPG in GC for the first time.

INTRODUCTION

Gastric cancer (GC) has high morbidity and mortality rates worldwide [1]. The incidence of GC varies greatly in different parts of the world, with high incidence in Asian countries, including China, Japan, and South Korea [1, 2]. More than one million new GC cases are reported annually, 40% of which occur in China. Most of the GC-related deaths also occur in China, which poses a serious threat to the health of Chinese people [1].

The comprehensive treatment for GC includes surgery, chemotherapy, radiotherapy, molecular targeted therapy, biological immunotherapy, and traditional Chinese medicine [3]. Despite the emergence of newer treatments, the recurrence and metastasis rates for advanced GC remain high, which leads to mortality in GC patients. Recurrence and metastasis in GC are complex, multi-step processes regulated by several genes, including oncogenes and tumor suppressor genes [4–6]. An understanding of the regulatory genes and

mechanisms of GC recurrence and metastasis may facilitate effective treatment.

Galectin-1 (Gal1) is one of the 15 members of the beta-galactose-binding proteins, galactoagglutinins. Recent studies have demonstrated that Gal1 is expressed in a variety of malignant tumors, including hepatocellular carcinomas [7], lung adenocarcinomas [8], pancreatic cancers [9], breast cancers [10], colon cancers [11], and GC [12]. It is mainly distributed in the extracellular matrix and cytoplasm, and regulates various biological activities of cancer cells. It promotes the occurrence, development, invasion, metastasis, angiogenesis, immune escape, and other biological functions of malignant tumors [13]. However, the mechanism by which Gal1 regulates the biological behavior of tumors is not completely understood.

Non-SMC condensin I complex, subunit G (NCAPG) is a mitotic gene located on human chromosome 4p15.32 and has a relative molecular weight of 114.1 kDa. Studies have shown that NCAPG expression varies among tissues, with high expression in testicular tissues and low expression in thymus. Its expression is also detectable in various tumors [14–17]. NCAPG overexpression is related to the proliferation and migration of hepatocellular carcinomas [18]. NCAPG expression is significantly higher in GC compared to the adjacent tissues, and it influences the prognosis of GC patients [19]. However, the association between NCAPG and Gal1 in GC patients has not been reported.

The present study focused on the role of Gal1 and NCAPG in GC and their effects on invasion and metastasis. We demonstrated that Gal1 and NCAPG could be used as predictors of GC prognosis. Their combination as a novel predictor had a high accuracy for survival assessment.

MATERIALS AND METHODS

Patient information and tissue samples

A total of 145 gastric adenocarcinoma patients, with detailed pathological and follow-up data were enrolled in this study. All patients were treated with radical gastrectomy and D2 lymphadenectomy at the Gastrointestinal Surgery Department, Taizhou People's Hospital of Jiangsu province between January 2015 and May 2017. No patient received radiotherapy or chemotherapy prior to surgery, had no serious diseases or other synchronous malignancies, or distant metastases prior to surgery. Overall survival (OS) and disease free survival (DFS) times were the primary

endpoints. OS was calculated from the date of surgery to the date of death or the final follow-up. DFS was calculated from the date of surgery to disease recurrence. The clinicopathological features of the patients are described in Table 1. Primary GC tissues (GCTs) and matched normal gastric mucosa tissues (NGCTs) were formalin-fixed and paraffin-embedded for hematoxylin and eosin (HE) staining and immunohistochemistry (IHC), while fresh GCTs and NGCTs were collected from eight patients for molecular analysis in April 2022.

IHC staining

Formalin-fixed, paraffin-embedded specimens were used for IHC analysis. The specimens were sliced at 4- μ m thickness. Xylene and gradient ethanol were used to deparaffinize and rehydrate the tissues. Endogenous peroxidases were blocked in methanol for 10 min using 3% hydrogen peroxide. Phosphate-buffered saline (PBS) was used to wash the slides three times, and citrate buffer (pH 6.0) was used for antigen retrieval for 20 min at 95°C. Rabbit monoclonal antibodies, anti-Gal1 (dilution, 1:250, Abcam, Cambridge, UK) and NCAPG (dilution, 1:200, Abcam), were incubated with the slides overnight at 4°C. The slides were washed thrice with PBS and incubated with biotin-conjugated secondary antibodies, followed by horseradish peroxidase-conjugated streptavidin. The sections were then stained with diaminobenzidine, counterstained with hematoxylin, dehydrated, cleared, and cover-slipped.

IHC analysis

Two pathologists, who were blinded to the clinical data, scored the IHC staining for Gal1 and NCAPG in GCTs and NGCTs using semi-quantitative immunoreactivity scores (IRS). Immunostaining intensity was documented as category A with scores of 0–3 (0, negative; 1, weak; 2, moderate; and 3, strong). The percentage of immunoreactive cells was documented as category B with scores of 1–4 (1, 0–25%; 2, 26–50%; 3, 51–75%; and 4, 76–100%). IRS was calculated by multiplying the scores for categories A and B, ranging from 0 to 12. Receiver operating characteristic (ROC) analysis was used to obtain the optimum cutoff values for IRS and to distinguish high and low expression of Gal1 and NCAPG.

Cell lines and culture

Human GC cells, SGC-7901 (Cat No. C6795), and undifferentiated GC cells, HGC-27 (Cat No. C6365), were provided by Shanghai Biyuntian Biological Co., Ltd. (Shanghai, China). RPMI-1640 (Gibco-BRL, Gaithersburg, MD, USA) with 10% (v/v) fetal bovine

Table 1. Relationship between expression levels of Gal1 or NCAPG and clinicopathological features in patients with GC.

All patients	Gal1		P	NCAPG		P
	High (%) n = 83	Low (%) n = 62		High (%) n = 110	Low (%) n = 35	
Sex			0.142			0.019
Male	52 (62.7)	46 (74.2)		80 (72.7)	18 (51.4)	
Female	31 (37.3)	16 (25.8)		30 (27.3)	17 (48.6)	
Age (years)			0.765			
>65	45 (54.2)	32 (51.6)		59 (53.6)	18 (51.4)	0.82
≤65	38 (45.8)	30 (48.4)		51 (46.4)	17 (48.6)	
Tumor diameter (cm)			0.004			0.027
>5	35 (42.2)	12 (19.4)		41 (37.3)	6 (17.1)	
≤5	48 (57.8)	50 (80.6)		69 (62.7)	29 (82.9)	
Pathological classification			<0.001			
I-II	7 (8.4)	31 (50.0)		16 (14.5)	22 (62.9)	0.001
III	76 (91.6)	31 (50.0)		94 (85.5)	13 (37.1)	
Depth of invasion			0.01			
T2-T3	9 (10.8)	17 (27.4)		14 (12.7)	12 (34.3)	0.004
T4	74 (89.2)	45 (72.6)		96 (87.3)	23 (65.7)	
Lymph node metastasis			0.001			0.037
N0	21 (25.3)	34 (54.8)		35 (31.8)	20 (57.2)	
N1	15 (18.1)	9 (14.5)		18 (16.4)	6 (17.1)	
N2	17 (20.5)	11 (17.8)		24 (21.8)	4 (11.4)	
N3	30 (36.1)	8 (12.9)		33 (30.0)	5 (14.3)	
TNM stage			0.011			
I	4 (4.8)	13 (21.0)		9 (8.2)	8 (22.9)	0.015
II	5 (6.0)	4 (6.4)		5 (4.5)	4 (11.4)	
III	74 (89.2)	45 (72.6)		96 (87.3)	23 (65.7)	

serum (Gibco-BRL), 100 mg/mL of streptomycin, and 100 U/mL of penicillin (Gibco-BRL) were used to culture GC cells. All cells were cultured in a humidified atmosphere containing 5% (v/v) CO₂ at 37°C, and passaged by trypsinization when 80% confluence was reached.

Lentiviral transduction

A lentiviral vector for *LGALS1* overexpression and a corresponding non-targeting negative control lentiviral vector were constructed by Genechem Co., Ltd. (Shanghai, China). The GV358 (Ubi-MCS-3FLAG-SV40-EGFP-IRES-puromycin) lentiviral vector was constructed to upregulate *LGALS1* expression. SGC-7901 and HGC-27 cells were seeded at a concentration of 5×10^4 cells per well in six-well plates before lentiviral transduction. The cells were transduced with lentiviral vector and 10 μg/mL

of polybrene (Sigma-Aldrich, St. Louis, MO, USA) based on an infection multiplicity of 10. The corresponding non-targeting negative control lentiviral vector was transduced through the same approach. The medium was replaced 12 h after transduction and puromycin (Sigma-Aldrich) was added to select stable transduced cell lines at the concentration of 2 μg/mL after another 48 h. The stable transduced cells were then cultured in the presence of 0.5 μg/mL of puromycin. Fluorescent microscopy (OLYMPUS-U-HGLGPS-IX73), qualitative reverse-transcriptase polymerase chain reaction (qRT-PCR), and Western blotting were used to evaluate transduction efficiency after 72 h.

siRNA transduction

The siRNA against *NCAPG* and matched negative control siRNA were purchased from Biomics

Biotechnologies Co. Ltd. (Nantong, China). OE-*LGALS1* SGC-7901 and OE-*LGALS1* HGC-27 cells were seeded in six-well plates at a concentration of 5×10^4 , and were transfected with *NCAPG* siRNA or control siRNA using Lipofectamine 2000 (Invitrogen, Carlsbad, CA, USA). The manufacturer's instructions were followed for all the steps. After 24 h, the cells were harvested for further experiments. The three siRNA sequences were as follows: hs-*NCAPG*-si-1 sense (5'-3'): CACGAUGGAUGAU AAGACA, hs-*NCAPG*-si-1 antisense (3'-5'): UGUCUUAUCAUCCA UCGUG; hs-*NCAPG*-si-2 sense (5'-3'): GGAGUUCA UUCAUACC UU, hs-*NCAPG*-si-2 antisense (3'-5'): AAGGUA AUGAAUGAACUCC; hs-*NCAPG*-si-3 sense (5'-3'): GCUGAAACA UUGCAGAAAU, and hs-*NCAPG*-si-3 antisense (3'-5'): AUUUCUGCAAUGUU UCAGC.

Wound healing assay

All cells were seeded in six-well plates at concentrations of 1×10^5 . When the cell monolayer reached a confluence of 80–90%, a 10- μ L pipette tip was scored across it to create a wound. PBS (Corning, Manassas, VA, USA) was used to wash the plates and remove cellular debris. The cells were photographed using a Leica DMIRB microscope (100 \times magnification; Leica, Wetzlar, Germany). Then, the cells were incubated with a serum-free medium containing 10 μ g/mL of mitomycin C to block proliferation, and the wounds were photographed after 24 h. The number of migrated wild type cells was defined as 100% to calculate the percentage of cell migration.

In vitro invasion assay

The invasion ability of SGC-7901 and HGC-27 cells was measured using 24-well transwell units with polycarbonate filters (pore size, 8.0 μ m; Corning, NY, USA). Matrigel[®] basement membrane (BD Biosciences, San Diego, CA, USA) was mixed with the serum-free RPMI at a ratio of 1:8, and 100 μ L of the mixture was used to coat the upper transwell inserts. Then, the cells were seeded at 1×10^5 in the upper insert with 100 μ L serum-free RPMI medium, and placed in the lower chambers with 600 μ L of complete media. The cells were allowed to culture for 24 h at 37°C, and non-invasive cells were removed using a cotton swab. The filters were fixed using 4% (v/v) paraformaldehyde, the cells were stained with 0.05% (v/v) crystal violet solution, and counted under a microscope.

RNA extraction and real-time PCR

The RNeasy Mini Kit (Invitrogen) was used to isolate real-time PCR RNAs, and the Revert Aid RT reverse

transcription kit (Thermo Fisher Scientific, Waltham, MA, USA) was used to reverse-translate the purified RNAs into cDNA. A SYBR Green dye kit (RocheDiagnostics, Mannheim, Germany) was used to perform qRT-PCR, and the products were analyzed using an iQ5 Multicolor real-time PCR Detection System (Bio-Rad, Hercules, CA, USA). GAPDH was used as the reference control gene and analyzed using the $2^{-\Delta\Delta C_t}$ method. The following primers were used: *NCAPG* (forward): ACCCAAGCATCAAAGTCTACT CAGC and (reverse) TGACACCTCTGTTCGTCTT AGC; *LGALS1* (forward): GCCAGATGGATACGAAT TCAAG and GCCACACATTTGATCTTGAAGT; and *GAPDH* (forward) CCAGCAAGAGCACAAAGAGGAA GAG and (reverse) GGTCTACATGGCAACTGTGA GGAG.

Western blotting

The tissues and cells were lysed using the RIPA buffer (Thermo Fisher Scientific) to prepare total cells extracts. Denatured proteins were separated by 10% sodium dodecyl sulfate-polyacrylamide gel electrophoresis (SDS-PAGE) and the separated proteins were transferred onto nitrocellulose membranes (GE Healthcare Life Sciences, Pittsburgh, PA, USA). Antibodies against Gall1, *NCAPG*, and *GAPDH* (dilution, 1:2000) were used to probe the proteins on the blots at 4°C overnight. They were then incubated with peroxidase-conjugated secondary anti-bodies (Sigma-Aldrich), and a West Pico chemiluminescent substrate (Pierce, Carlsbad, CA, USA) was used to visualize the immunoreactive protein bands. A densitometric image analysis software (Image Master VDS; Pharmacia Biotech, Little Chalfont, UK) was used to quantify the proteins. *GAPDH* levels were determined as an internal reference. All experiments were independently performed thrice.

Statistical analyses

SPSS Statistics version 25.0 software (IBM Corp., Armonk, NY, USA) was used to analyze the data. The clinicopathological features and protein expression levels were compared using the chi-square test. Wilcoxon test (grouped) was used to analyze the IRS for Gall1 and *NCAPG* in GCTs and NGCTs. OS and DFS were analyzed through Kaplan-Meier survival analysis. The hazard ratios (HRs) and 95% confidence intervals (CIs) were estimated by univariate or multivariate Cox regression analysis. Continuous variables were expressed as means \pm standard error of the mean. Multiple comparisons were performed through one-way analysis of variance (ANOVA) and Dunnett's *t* test. *P*-values < 0.05 were considered significant.

RESULTS

Gall1 and NCAPG expression in GC and non-cancer tissues

Western blotting was used to analyze Gall1 and NCAPG expressions in eight paired specimens from GC patients, including primary GCTs and matched NGCTs. GCTs had increased Gall1 and NCAPG expressions compared to the paired NGCTs (Figure 1A, 1B). Immunohistochemistry of the GCTs and NGCTs was used to further investigate Gall1 and NCAPG expressions in 145 primary GC patients. Gall1 staining was mainly localized in the cytoplasm and extracellular matrix, whereas NCAPG was mainly expressed in the cytoplasm and nuclei (Figure 1C). Typical images of Gall1 and NCAPG expression in non-cancer tissues are shown in Figure 1D. The IRS distribution for Gall1 and NCAPG expressions in primary GCTs and NGCTs are shown in Figure 1E, 1F. Compared to NGCTs, Gall1 and NCAPG expressions in GCTs were significantly increased (both $P < 0.001$, Figure 1E, 1F). NCAPG expression correlated significantly with Gall1 expression in cancerous tissues ($r = 0.653$, $P < 0.001$, Figure 1G).

Gall1 and NCAPG expression correlated with clinicopathological characteristics

IHC cutoff scores were used to classify Gall1 and NCAPG levels as high and low through ROC analysis. $IRS \geq 9.17$ and ≥ 3.17 indicated high Gall1 (Figure 2A) and NCAPG (Figure 2B) expressions, respectively. Based on this standard, high Gall1 and NCAPG expression was 83 (57.24%) and 110 (75.86%) in GC cases, respectively. Gall1 expression in GCTs correlated with the clinicopathological features (Table 1), including tumor diameter, pathological classification, depth of invasion, lymph node metastasis, and TNM stage (all $P < 0.05$). NCAPG expression in GCTs was significantly associated with gender, tumor diameter, pathological classification, depth of invasion, lymph node metastasis, and TNM stage (all $P < 0.05$).

High Gall1 and NCAPG expression inversely correlated with survival

All patient follow-up ended at death or at least 5 years, the median follow-up time was 36.37 months. Kaplan-Meier analysis revealed that high Gall1 or NCAPG expression in GCTs was significantly correlated with poor OS (all $P < 0.001$, Figure 2C, 2D) and DFS (all $P < 0.001$, Figure 2F, 2G). Univariate Cox regression

analysis indicated that tumor diameter, pathological classification, depth of invasion, lymph node metastasis, TNM stage, and Gall1 and NCAPG expression were associated with OS in GC patients (all $P < 0.001$, Table 2). Multivariate Cox regression analysis indicated that tumor diameter, TNM stage, Gall1 and NCAPG expression were independent prognostic factors for GC (Gall1: HR, 0.072, 95% CI, 0.035–0.145, $P < 0.001$; NCAPG: HR, 0.185, 95% CI, 0.081–0.420, $P < 0.001$, Table 3).

Synergistic effect of Gall1 and NCAPG on OS and DFS

The patients were stratified into three groups based on the IRS for Gall1 and NCAPG, i.e., both high ($n = 73$), either Gall1 or NCAPG high ($n = 47$), and both low ($n = 25$). Kaplan-Meier analysis revealed that the both low expression group had more favorable OS and DFS, while the both high expression group had poorer OS and DFS, compared to the Gall1 or NCAPG high group ($P < 0.001$, Figure 2E, 2H).

Gall1 regulates NCAPG at mRNA and protein levels

We constructed lentivirus that overexpressed *LGALS1* in SGC-7901 and HGC-27 cells to obtain four cell lines, overexpressed LV-*LGALS1* SGC-7901 (OE-*LGALS1* SGC-7901), overexpressed LV-*LGALS1* HGC-27 (OE-*LGALS1* HGC-27), and corresponding transfected negative control (NC) cells. Successful overexpression of *LGALS1* was confirmed by green fluorescent protein signal (Figure 3A, 3B), Western blotting (Figure 3C, 3D), and qRT-PCR (Figure 3E, 3F). Western blotting indicated that OE-*LGALS1* SGC-7901 and OE-*LGALS1* HGC-27 cells had higher Gall1 levels than NC cells and wild cells ($P < 0.05$ and < 0.01 , respectively, Figure 3C, 3D). mRNA expression for *LGALS1* was detected using qRT-PCR; the expression of *LGALS1* mRNA was consistent with Gall1 protein expression (all $P < 0.01$, Figure 3E, 3F).

In all cell lines, NCAPG expression was consistent with Gall1 expression on Western blotting, and was significantly higher in OE-*LGALS1* GC cells than in NC cells and wild cells (all $P < 0.01$, Figure 3C, 3D). We then performed qRT-PCR to evaluate *NCAPG* mRNA expression in all cell lines, and the results were consistent with those of Western blotting (all $P < 0.01$, Figure 3E, 3F). This indicated that *LGALS1* could positively regulate *NCAPG* expression at mRNA and protein levels.

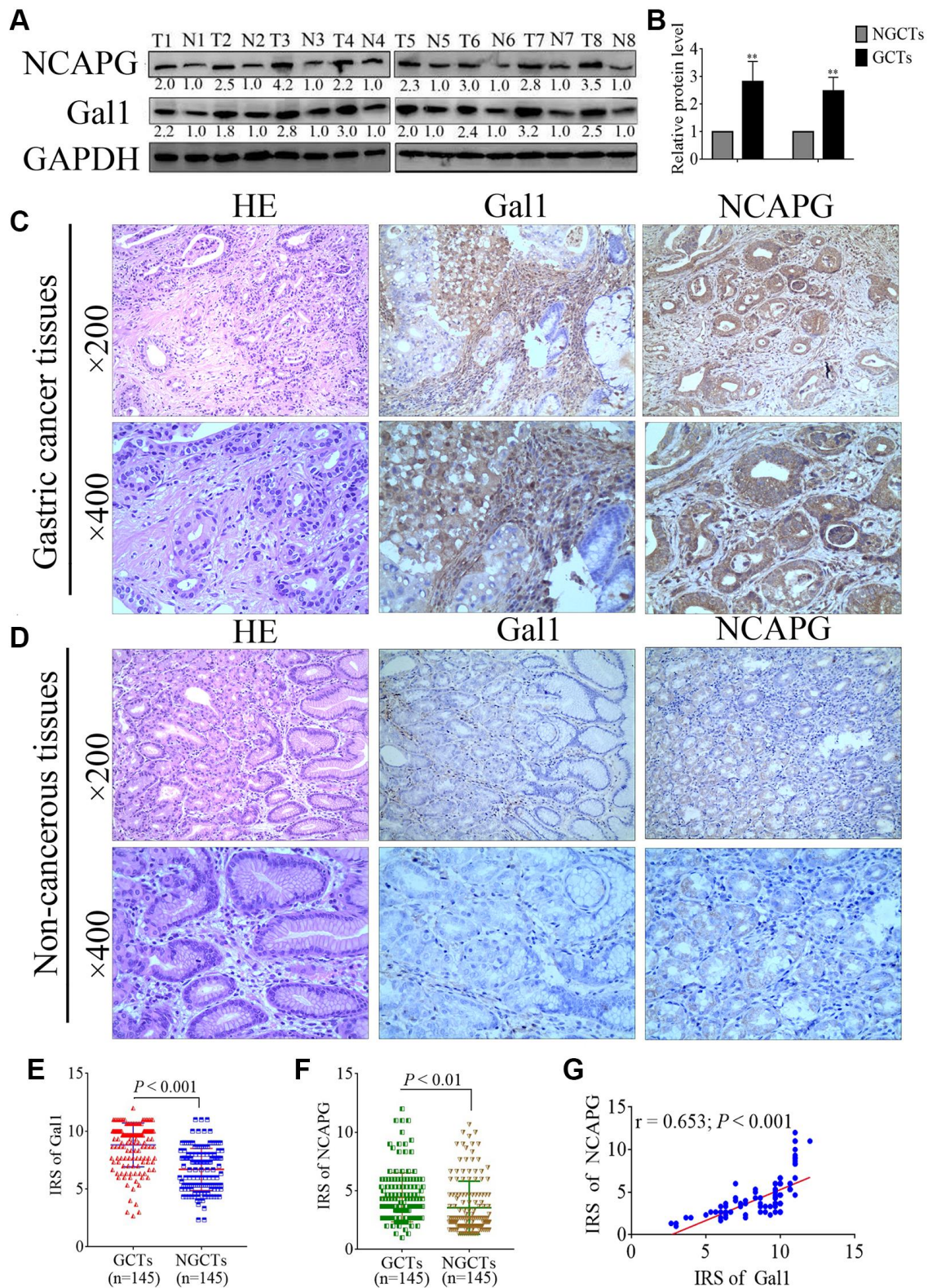


Figure 1. Gal1 and NCAPG expression predict prognosis of gastric cancer (GC). (A, B) Expression of Gal1 and NCAPG proteins detected by Western blotting in GC cancer tissues (GCTs) and non-gastric cancer tissues (NGCTs). (C, D) Representative immunohistochemistry images for Gal1 and NCAPG in (C) GC tissues, and (D) matched non-cancerous tissues. (E) Immunoreactivity score (IRS) for Gal1 compared between GCTs and matched NGCTs. (F) IRS for NCAPG compared between GCTs and matched NGCTs. (G) The expression of Gal1 was positively correlated with NCAPG expression in GC tissues. Abbreviations: T: tumor tissue; N: non-tumor tissue; GCTs: gastric cancer tissues; NGCTs: non-gastric cancer tissues. ** $P < 0.01$.

LGALS1 and NCAPG mutually reinforced GC cell line regulation

In order to further explore the regulatory relationship between *LGALS1* and *NCAPG*, lentiviral was used to generate overexpressed LV-*LGALS1* SGC-7901 and HGC-27 stable cell lines. We constructed an siRNA to simultaneous silence *NCAPG* expression in these stable cell lines, and obtained OE-*LGALS1*+ *NCAPG*-knockdown GC cells (OE-*LGALS1*+si*NCAPG*), including both SGC-7901 and HGC-27 cell lines. mRNA expressions for *LGALS1* and *NCAPG* were detected using qRT-PCR. *NCAPG* knockdown in

OE-*LGALS1* GC cell lines significantly inhibited *NCAPG* mRNA expression for SGC-7901 ($P < 0.01$, Figure 4A) and HGC-27 ($P < 0.01$, Figure 4B). However, *LGALS1* mRNA expression was also decreased when *NCAPG* was knocked down in OE-*LGALS1* GC cell lines, including SGC-7901 ($P < 0.01$, Figure 4C) and HGC-27 ($P < 0.01$, Figure 4D). Thus, *LGALS1* and *NCAPG* mutually reinforced GC cell line regulation. In order to further verify these results, Western blotting was used to detect Gal1 and *NCAPG* protein expressions in each GC cell line, and the results were consistent with those of qRT-PCR (all $P < 0.01$, Figure 4E, 4F).

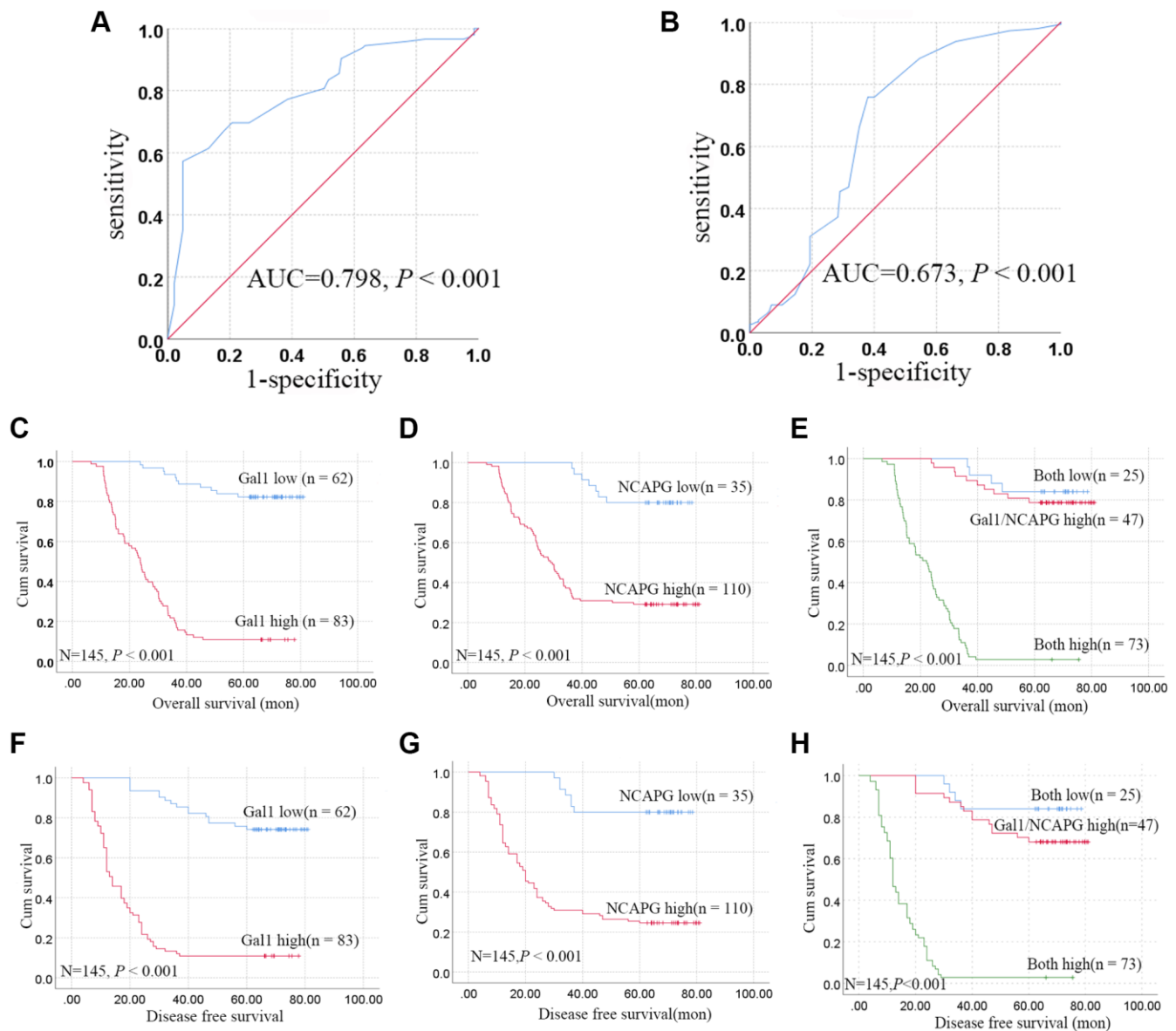


Figure 2. Aberrant Gal1 and NCAPG expression in GC tissues indicates poor prognosis. (A, B) Receiver operating characteristic statistics were employed to estimate the cut-off points of the IRS for (A) Gal1 and (B) NCAPG in GC tissues. (C–E) Kaplan-Meier curves for Gal1, NCAPG, and combined Gal1/NCAPG expression in the training cohort for overall survival. (F–H) Kaplan-Meier curves for Gal1, NCAPG, and combined Gal1/NCAPG expression in the training cohort for disease free survival.

Table 2. Univariate Cox regression analysis of clinicopathological variables, Gal1 and NCAPG in patients with GC.

Variable	<i>n</i> = 145	
	HR (95% CI)	<i>P</i>
Sex (male vs. female)	0.909 (0.580–1.423)	0.675
Age (≤65 years vs. >65 years)	1.211 (0.788–1.860)	0.382
Tumor diameter (≤5 cm vs. >5 cm)	3.117 (2.022–4.805)	<0.001
Pathological classification (I/II vs. III)	1.810 (0.789–4.153)	<0.001
Depth of invasion (T2/T3 vs. T4)	5.447 (2.203–13.473)	<0.001
Lymph node metastasis (N0 vs. N1–N3)	1.454 (1.221–1.731)	<0.001
TNM stage (I–II vs. III)	0.184 (0.074–0.454)	<0.001
Gal1 state (low vs. high)	12.825 (6.704–24.534)	<0.001
NCAPG state (low vs. high)	6.325 (2.908–13.757)	<0.001

Table 3. Multivariate Cox regression analysis of clinicopathological variables, Gal1 and NCAPG expression in patients with GC.

Variable	B	<i>n</i> = 145		
		Wald	HR (95% CI)	<i>P</i>
Tumor diameter (≤5 cm vs. >5 cm)	–0.691	8.579	0.501 (0.316–0.795)	0.003
TNM stage (I–II vs. III)	–2.670	6.868	0.069 (0.009–0.510)	0.009
Gal1 state (low vs. high)	–2.632	53.153	0.072 (0.035–0.145)	<0.001
NCAPG state (low vs. high)	–1.689	16.235	0.185 (0.081–0.420)	<0.001

LGALS1 promoted migration and invasion in GC cells through NCAPG regulation

Wound healing and transwell assays were used to assess migration and invasion abilities of SGC-7901 and HGC-27 cells, and compare them to the NC (OE-*LGALS1* transfected NCs), OE-*LGALS1*, and OE-*LGALS1*+siNCAPG groups. The wound healing experiment demonstrated that *LGALS1* overexpression enhanced SGC-7901 migration. However, this was partly rescued by reinfected *NCAPG*-siRNA in OE-*LGALS1* GC cells (Figure 5A). Figure 5B shows the fold changes in migration. These experiments were repeated in HGC-27 cells to confirm *LGALS1*-mediated promotion of migration *in vitro*, which was reduced by simultaneous *NCAPG*-knockdown (Figure 5C, 5D).

Transwell assay showed significantly enhanced invasion ability in OE-*LGALS1*, SGC-7901, and HGC-27 cells. The cell invasion capability could be partly rescued by re-infected *NCAPG*-siRNA in OE-*LGALS1* GC cells (Figure 5E; *P* < 0.01).

DISCUSSION

GC has a very high mortality rate, with over a million new cases and 769,000 estimated deaths reported in 2020 [1]. In China, approximately 80% of the patients diagnosed with GC have advanced metastatic disease [20]. This is because of the lack of non-invasive

examination methods and sensitive screening markers. Although the long-term survival rate for GC patients has improved in China since 2000 [21], it still remains unsatisfactory [22]. Recurrence and metastasis after surgery are the main causes of death in advanced GC. Although TNM staging is the gold standard for prognosis assessment of GC patients, it cannot accurately predict the risk of postoperative recurrence and metastasis. Therefore, there is an urgent need to develop novel methods for diagnosis, treatment, and prognosis evaluation for GC patients, and to provide therapeutic targets for targeted therapy.

Previous studies have found that Gal1 promotes cell shedding, homotype cell aggregation, migration, invasion, adhesion, and angiogenesis in tumors [13]. Previous studies have also demonstrated that high Gal1 expression in GC-associated fibroblasts induced epithelial-mesenchymal transition and enhanced GC cell invasion and metastasis [23].

Galactosectins play a variety of roles in normal physiology. In cancer, they are often expressed at elevated levels and associated with poor prognosis [24]. They are known to contribute to various cancer progression pathways by interacting with cancers and matrix glycans [24]. Research on the regulation of biological behavior of GC by galactosectins has focused on Gal1, Gal-3, and Gal-9 [24–26]. Previous studies have shown that Gal1 expression in GCTs is associated

with poor prognosis in GC patients [27, 28]. The present study showed that Gal1 was significantly higher in GCTs than in the adjacent non-cancerous tissues, and that its expression was correlated with tumor diameter,

pathological classification, depth of invasion, lymph node metastasis, and TNM stage. All these pathological parameters are also correlated with GC prognosis. Kaplan-Meier survival analysis showed that high Gal1

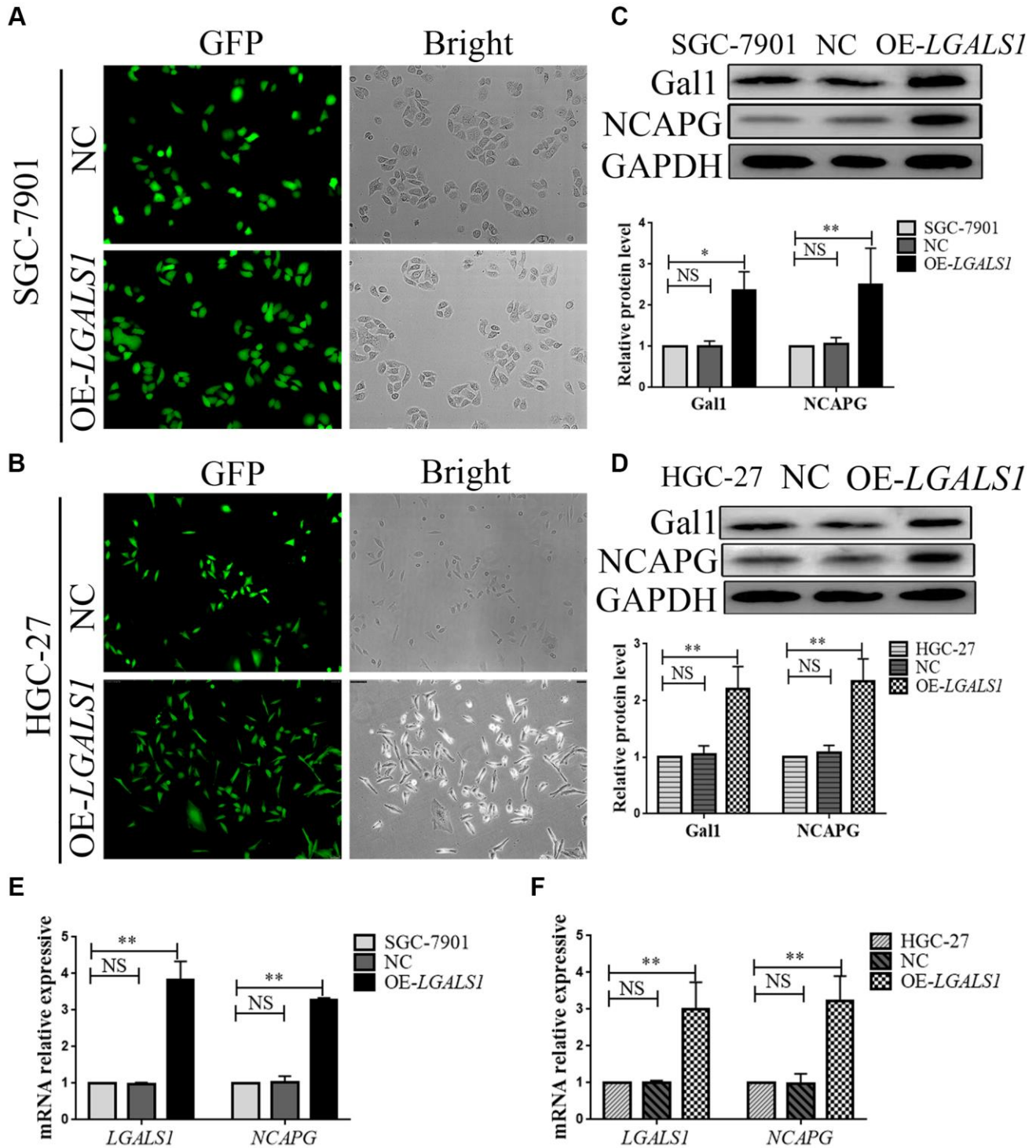


Figure 3. *LGALS1* regulates *NCAPG* at the mRNA and protein levels. Transduction efficiency confirmed by green fluorescent protein (GFP) assay in (A) SGC-7901 cells and (B) HGC-27 cells. Original magnification 200 \times . (C, D) Western blot confirmation of stable overexpression of Gal1 and NCAPG in (C) SGC-7901 and (D) HGC-27 cells when *LGALS1* was overexpressed. (E, F) Quantitative real-time PCR (qRT-PCR) analysis of *LGALS1* and *NCAPG* expression in (E) SGC-7901 and (F) HGC-27 cells when *LGALS1* was overexpressed. Abbreviations: OE-*LGALS1*: Overexpression of *LGALS1*; NC: negative control (empty vector); NS: not significant. * $P < 0.05$; ** $P < 0.01$.

expression in GCTs was significantly correlated with postoperative OS and DFS in GC patients. These results suggest that Gal1 expression may regulate the malignant biological behavior of GCTs and is closely

related to patient prognosis. Therefore, Gal1 may be used as an indicator for the prognosis of GC patients. However, the mechanism by which Gal1 affects GC prognosis has not been fully elucidated.

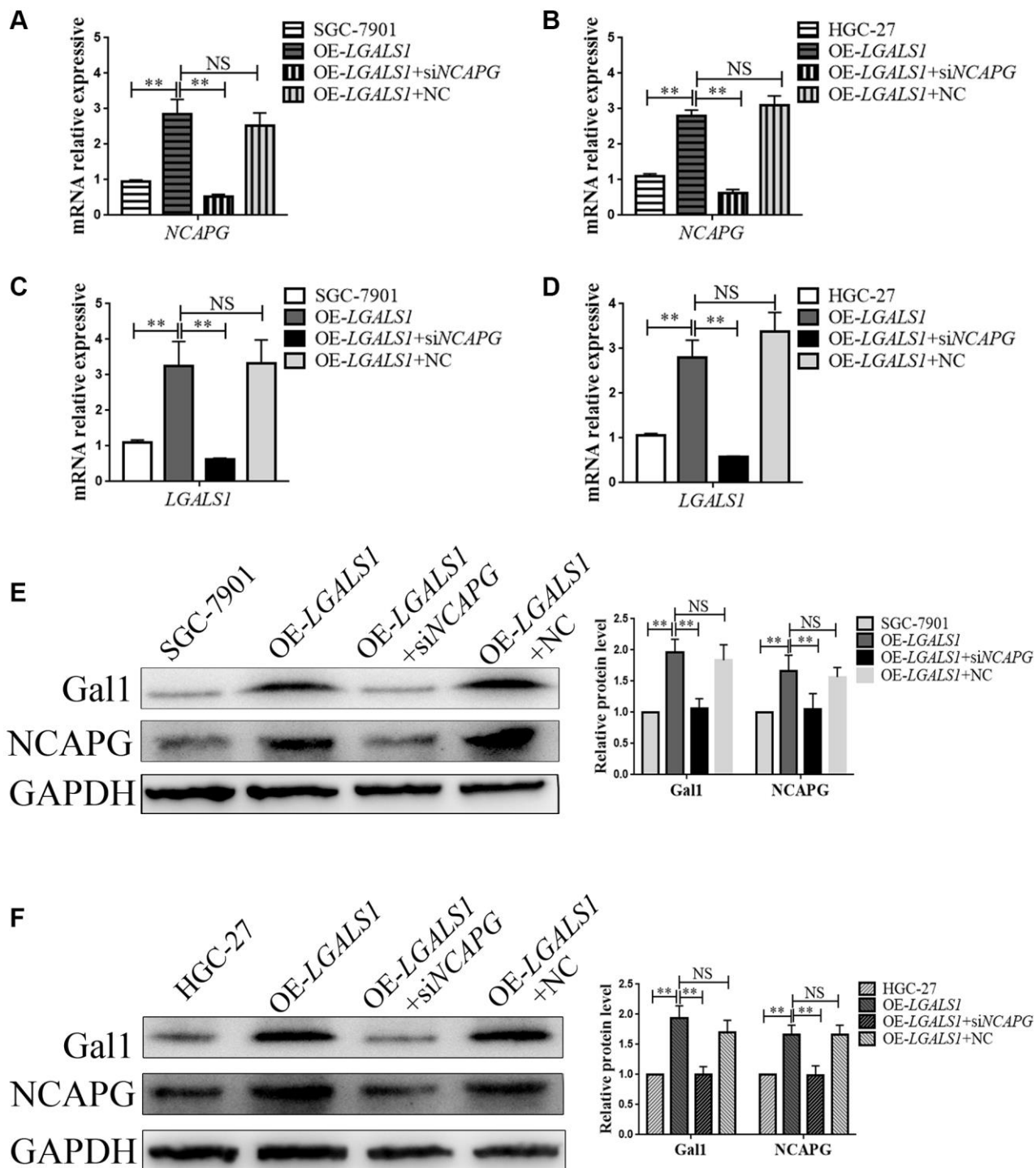


Figure 4. *LGALS1* and *NCAPG* may mutually reinforce regulation in GC cell lines. qRT-PCR analysis of (A, B) *NCAPG* and (C, D) *LGALS1* expression in SGC-7901 and HGC-27 cells when *LGALS1* was overexpressed, with or without simultaneous silencing of *NCAPG*. Western blot confirmation of stable overexpression of Gal1 and *NCAPG* in (E) SGC-7901 and (F) HGC-27 cells when *LGALS1* was overexpressed, with or without simultaneous silencing of *NCAPG*. Abbreviations: OE-*LGALS1*: Overexpression of *LGALS1*; siNCAPG: silencing of *NCAPG*; OE-*LGALS1*+NC: overexpression of *LGALS1* + *NCAPG* negative control (empty vector); NS: not significant. **P* < 0.05; ***P* < 0.01.

In this study, we found that Gal1 expression in GCTs was closely related to NCAPG expression, which has not been reported in previous studies. NCAPG is a subunit of the agglutinate protein complex that is responsible for chromosomal cohesion and stability

during cell division [29]. According to gene ontology analyses, NCAPG-related pathways include the cell cycle, mitosis, and cell-cycle chromosome premetaphase coagulation. Previously, RNA-seq was performed on tissue samples from 95 human individuals,

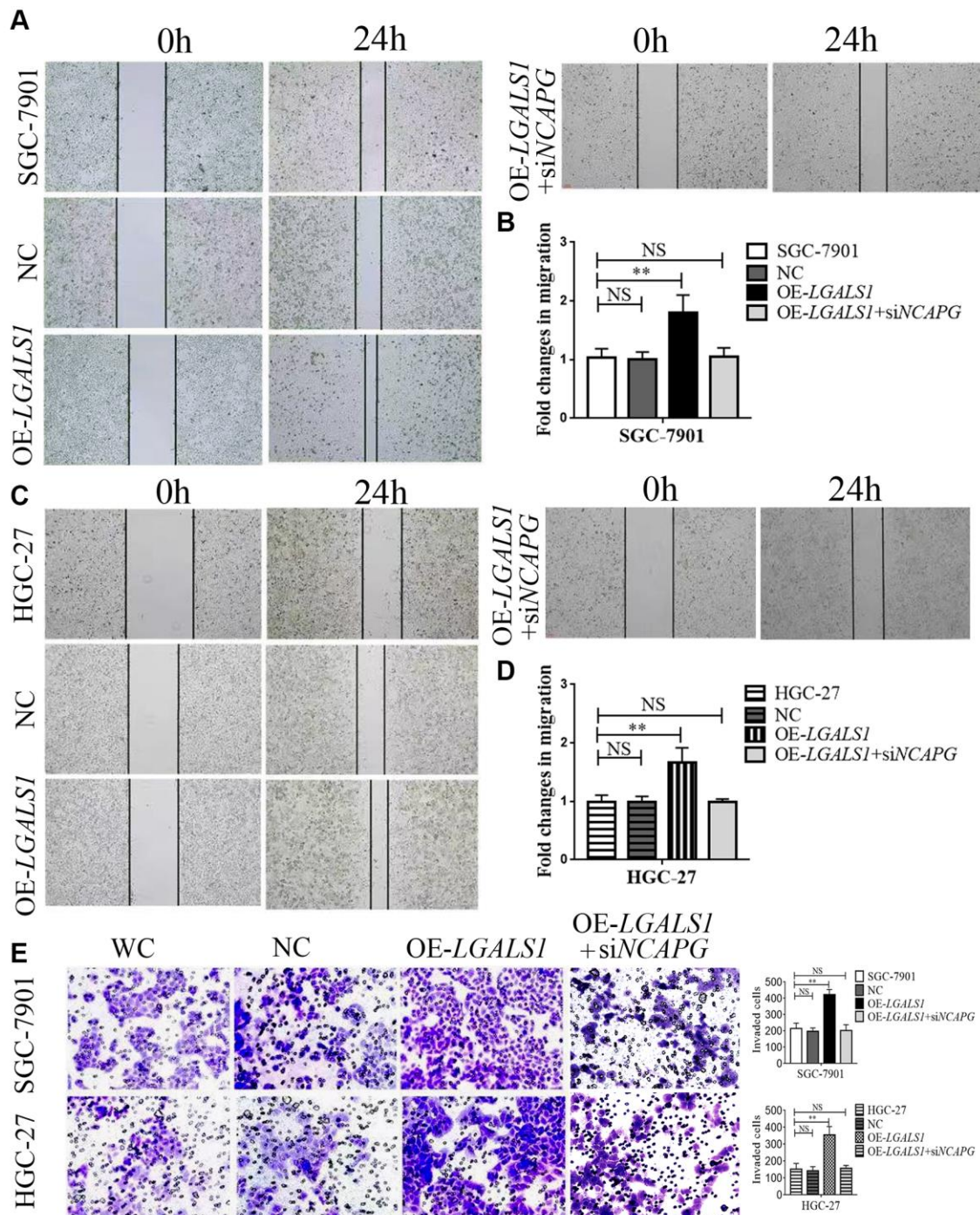


Figure 5. *LGALS1* promotes the migration and invasion of GC cell lines *in vitro*. Overexpression of *LGALS1* (OE-*LGALS1*) significantly enhanced the migration capacity of (A, B) SGC-7901 and (C, D) HGC-27 cells compared with wild control (WC) and negative controls (NC). The migration capacity was abolished when *NCAPG* was simultaneously silenced. Magnification: $\times 100$. (E) Transwell assay showing that overexpressed *LGALS1* significantly enhanced the invasion ability of SGC-7901 and HGC-27 cells, and simultaneous silencing of *NCAPG* abolished the invasion capacity ($n = 3$). Magnification: $\times 200$. Abbreviations: NC: negative control (empty vector); OE-*LGALS1*: Overexpression *LGALS1*; OE-*LGALS1*+siNCAPG: Overexpression of *LGALS1* +silencing of *NCAPG*. NS: not significant. $^{**}P < 0.01$.

representing 27 different tissues, in order to determine the tissue specificity of the protein-coding genes [30]. NCAPG is mainly expressed in the bone marrow, lymph nodes, and testes in healthy individuals. Several recent studies have found abnormal NCAPG expression in a variety of tumors, including GC, which affects their prognosis [14, 15, 17, 18, 31]. It has been demonstrated that NCAPG expression in GCTs can predict the prognosis of GC patients [19]. However, the expression and functional role of NCAPG in GC remain unclear. We observed that NCAPG expression in GCTs was higher than in the adjacent tissues. NCAPG expression in GCTs was also positively correlated with gender, tumor diameter, pathological classification, depth of invasion, lymph node metastasis, and TNM stage. Although the association between gender and GC prognosis has not been reported, all the remaining factors are known prognostic indicators in GC patients. Furthermore, several gender-dependent diagnostic markers for GC have been reported, including Kindlin-1, an adhesion protein member of the integrin-interacting proteins [32]. Therefore, the relationship between NCAPG expression and gender in GC requires further analysis.

Kaplan-Meier survival analysis also showed that high Gal1 expression in GCTs was significantly correlated with postoperative OS and DFS, which was consistent with previous studies. Gal1 and NCAPG were also found to have a synergistic effect. Cox regression model confirmed that high Gal1 and NCAPG expressions were effective independent prognostic factors in all patient groups.

In order to explore the relationship between Gal1 and NCAPG, we conducted an *in vitro* experiment. We found that Gal1 regulated NCAPG expression at mRNA and protein levels. When we knocked down *NCAPG* in OE-*LGALS1* GC cells, Gal1 expression also decreased. This indicates that Gal1 and NCAPG may regulate each other. Existing literature suggests that *NCAPG* promotes oncogenesis in non-small cell lung cancer cells by upregulating *LGALS1* expression [14]. Our study was the first to demonstrate that *LGALS1* regulates *NCAPG* expression in GC, and that *LGALS1* and *NCAPG* may be mutually regulated. Further *in vitro* analysis confirmed that *LGALS1* promoted GC invasion and metastasis through *NCAPG* regulation.

The regulation of GC invasion and migration by NCAPG has also been reported previously [33]. NCAPG overexpression in GC cell lines decreased the levels of caspase-3, Bax, and E-cadherin, but elevated Bcl-2, vimentin, N-cadherin, Snail, and Slug levels. NCAPG overexpression also increased the

expression of Wnt1, phosphorylated GSK3beta, and total beta-catenin, while decreasing the expression of phosphorylated catenin. Functionally, NCAPG overexpression improved the anti-apoptotic ability of GC cells and promoted their Epithelial-mesenchymal Transition (EMT), making them more aggressive and mobile. In conclusion, NCAPG overexpression may promote EMT and inhibit tumor cell apoptosis by activating the Wnt/ β -catenin signaling pathway [33]. Several genes can promote GC metastasis by activating the Wnt/ β -catenin signaling pathway [34, 35]. In addition, Wnt/ β -catenin signaling pathway activation can also promote GC proliferation, apoptosis [36], and ferroptosis resistance [37]. However, the mechanism by which *LGALS1* regulates *NCAPG* has not been reported. Subsequent studies may explore these molecular mechanisms in GC cells through single-cell sequencing and other experiments to develop new therapeutic targets.

In summary, Gal1 and NCAPG could be prognostic molecular biomarkers for GC. Gal1 promotes GC cell invasion and migration through targeted regulation of NCAPG *in vitro*. Notably, the combination of Gal1 and NCAPG was an efficient prognostic indicator for GC and their synergistic effect is reported for the first time. Further investigations of the role of these proteins may provide new opportunities for novel GC treatment strategies.

AUTHOR CONTRIBUTIONS

Xiaolan You and Tingrui Zheng conceptualized the project and designed the experiments. Tao Qian and Haihua Zhou collected data of included patients. Tao Qian, Zhiyi Cheng, Guiyuan Liu, and Chuanjiang Huang prepared samples. Tingrui Zheng, Rongrong Dou, and Fuxing Liu performed all the experimental work. Xiaolan You, Tingrui Zheng and Tao Qian performed statistical analysis of data. Xiaolan You and Tingrui Zheng designed the tables and figures. Tingrui Zheng drafted this manuscript, which was reviewed by Xiaolan You. All authors read and approved the final manuscript.

ACKNOWLEDGMENTS

The authors would like to thank the native English-speaking scientists of Elixigen Company (Huntington Beach, CA, USA) for editing our manuscript.

CONFLICTS OF INTEREST

The authors declare no conflicts of interest related to this study.

ETHICAL STATEMENT AND CONSENT

The study was performed in accordance with the Declaration of Helsinki and approved by the Clinical Research Ethics Committee of Taizhou People's Hospital (KY2023-001-01), and written informed consent was obtained from all patients. We registered the study in the Chinese Clinical Trial Registry, Clinical Trial Registration Number- ChiCTR2300070242.

FUNDING

This work was supported by the Natural Science Foundation of Jiangsu Province, China (grant number BK20201230), and the Taizhou Fifth Phase 311 Talent Training Project (grant number RCPY202022).

REFERENCES

1. Sung H, Ferlay J, Siegel RL, Laversanne M, Soerjomataram I, Jemal A, Bray F. Global Cancer Statistics 2020: GLOBOCAN Estimates of Incidence and Mortality Worldwide for 36 Cancers in 185 Countries. *CA Cancer J Clin.* 2021; 71:209–49. <https://doi.org/10.3322/caac.21660> PMID:33538338
2. Ning FL, Lyu J, Pei JP, Gu WJ, Zhang NN, Cao SY, Zeng YJ, Abe M, Nishiyama K, Zhang CD. The burden and trend of gastric cancer and possible risk factors in five Asian countries from 1990 to 2019. *Sci Rep.* 2022; 12:5980. <https://doi.org/10.1038/s41598-022-10014-4> PMID:35395871
3. Hamashima C. The burden of gastric cancer. *Ann Transl Med.* 2020; 8:734. <https://doi.org/10.21037/atm.2020.03.166> PMID:32647659
4. Wang S, Chen X, Fu Y, Zhang H, Liu W, Song X, Ma X, Cheng S, Lu J. Relationship of ERCC5 genetic polymorphisms with metastasis and recurrence of gastric cancer. *Rev Assoc Med Bras (1992).* 2021; 67:1538–43. <https://doi.org/10.1590/1806-9282.20210209> PMID:34909875
5. Takeuchi A, Ojima T, Katsuda M, Hayata K, Goda T, Kitadani J, Tominaga S, Fukuda N, Nakai T, Yamaue H. Venous Invasion Is a Risk Factor for Recurrence of pT1 Gastric Cancer with Lymph Node Metastasis. *J Gastrointest Surg.* 2022; 26:757–63. <https://doi.org/10.1007/s11605-021-05238-0> PMID:35013879
6. Zeng CDD, Jin CC, Gao C, Xiao AT, Tong YX, Zhang S. Preoperative Folate Receptor-Positive Circulating Tumor Cells Are Associated With Occult Peritoneal Metastasis and Early Recurrence in Gastric Cancer Patients: A Prospective Cohort Study. *Front Oncol.* 2022; 12:769203. <https://doi.org/10.3389/fonc.2022.769203> PMID:35425708
7. Carabias P, Espelt MV, Bacigalupo ML, Rojas P, Sarrias L, Rubin A, Saffioti NA, Elola MT, Rossi JP, Wolfenstein-Todel C, Rabinovich GA, Troncoso MF. Galectin-1 confers resistance to doxorubicin in hepatocellular carcinoma cells through modulation of P-glycoprotein expression. *Cell Death Dis.* 2022; 13:79. <https://doi.org/10.1038/s41419-022-04520-6> PMID:35075112
8. Huang CC, Chuang IC, Su YL, Luo HL, Chang YC, Chen JY, Hsiao CC, Huang EY. Prognostic Significance of Galectin-1 but Not Galectin-3 in Patients With Lung Adenocarcinoma After Radiation Therapy. *Front Oncol.* 2022; 12:834749. <https://doi.org/10.3389/fonc.2022.834749> PMID:35280768
9. Tung CL, Lin MW, Hu RY, Chien YC, Liao EC, Lin LH, Chung TW, Wei YS, Tsai YT, Chen HY, Chou HC, Kuo WH, Ko ML, et al. Proteomic Analysis of Metastasis-Specific Biomarkers in Pancreatic Cancer: Galectin-1 Plays an Important Metastatic Role in Pancreatic Cancer. *J Pharm Biomed Anal.* 2020; 186:113300. <https://doi.org/10.1016/j.jpba.2020.113300> PMID:32413824
10. Balestrieri K, Kew K, McDaniel M, Ramez M, Pittman HK, Murray G, Vohra NA, Verbanac KM. Proteomic identification of tumor- and metastasis-associated galectin-1 in claudin-low breast cancer. *Biochim Biophys Acta Gen Subj.* 2021; 1865:129784. <https://doi.org/10.1016/j.bbagen.2020.129784> PMID:33166603
11. Park GB, Kim D. TLR4-mediated galectin-1 production triggers epithelial-mesenchymal transition in colon cancer cells through ADAM10- and ADAM17-associated lactate production. *Mol Cell Biochem.* 2017; 425:191–202. <https://doi.org/10.1007/s11010-016-2873-0> PMID:27837433
12. Naumova LA, Osipova ON, Klinnikova MG. Immunistochemical Analysis of the Expression of TGFβ, Galectin-1, Vimentin, and Thrombospondin in Gastric Cancer Associated with Systemic Undifferentiated Connective Tissue Dysplasia. *Bull Exp Biol Med.* 2019; 166:774–8. <https://doi.org/10.1007/s10517-019-04438-8> PMID:31028580
13. Cousin JM, Cloninger MJ. The Role of Galectin-1 in Cancer Progression, and Synthetic Multivalent

- Systems for the Study of Galectin-1. *Int J Mol Sci.* 2016; 17:1566.
<https://doi.org/10.3390/ijms17091566>
PMID:27649167
14. Sun H, Zhang H, Yan Y, Li Y, Che G, Zhou C, Nicot C, Ma H. NCAPG promotes the oncogenesis and progression of non-small cell lung cancer cells through upregulating LGALS1 expression. *Mol Cancer.* 2022; 21:55.
<https://doi.org/10.1186/s12943-022-01533-9>
PMID:35180865
 15. Zhou Y, Fan Y, Mao Y, Lou M, Liu X, Yuan K, Tong J. NCAPG is a prognostic biomarker of immune infiltration in non-small-cell lung cancer. *Biomark Med.* 2022; 16:523–35.
<https://doi.org/10.2217/bmm-2021-1090>
PMID:35199566
 16. Shi Y, Ge C, Fang D, Wei W, Li L, Wei Q, Yu H. NCAPG facilitates colorectal cancer cell proliferation, migration, invasion and epithelial-mesenchymal transition by activating the Wnt/ β -catenin signaling pathway. *Cancer Cell Int.* 2022; 22:119.
<https://doi.org/10.1186/s12935-022-02538-6>
PMID:35292013
 17. Tang F, Yu H, Wang X, Shi J, Chen Z, Wang H, Wan Z, Fu Q, Hu X, Zuhair Y, Liu T, Yang Z, Peng J. NCAPG promotes tumorigenesis of bladder cancer through NF- κ B signaling pathway. *Biochem Biophys Res Commun.* 2022; 622:101–7.
<https://doi.org/10.1016/j.bbrc.2022.07.007>
PMID:35843088
 18. Zhang Q, Su R, Shan C, Gao C, Wu P. Non-SMC Condensin I Complex, Subunit G (NCAPG) is a Novel Mitotic Gene Required for Hepatocellular Cancer Cell Proliferation and Migration. *Oncol Res.* 2018; 26:269–76.
<https://doi.org/10.3727/096504017X15075967560980>
PMID:29046167
 19. Sun DP, Lin CC, Hung ST, Kuang YY, Hseu YC, Fang CL, Lin KY. Aberrant Expression of NCAPG is Associated with Prognosis and Progression of Gastric Cancer. *Cancer Manag Res.* 2020; 12:7837–46.
<https://doi.org/10.2147/CMAR.S248318>
PMID:32922082
 20. Shu Y, Ding Y, Zhang Q. Cost-Effectiveness of Nivolumab Plus Chemotherapy vs. Chemotherapy as First-Line Treatment for Advanced Gastric Cancer/Gastroesophageal Junction Cancer/Esophageal Adenocarcinoma in China. *Front Oncol.* 2022; 12:851522.
<https://doi.org/10.3389/fonc.2022.851522>
PMID:35515123
 21. Li H, Zhang H, Zhang H, Wang Y, Wang X, Hou H, and Global Health Epidemiology Reference Group. Survival of gastric cancer in China from 2000 to 2022: A nationwide systematic review of hospital-based studies. *J Glob Health.* 2022; 12:11014.
<https://doi.org/10.7189/jogh.12.11014>
PMID:36527356
 22. Salati M, Ghidini M, Paccagnella M, Reggiani Bonetti L, Bocconi A, Spallanzani A, Gelsomino F, Barbin F, Garrone O, Daniele B, Dominici M, Facciorusso A, Petrillo A. Clinical Significance of Molecular Subtypes in Western Advanced Gastric Cancer: A Real-World Multicenter Experience. *Int J Mol Sci.* 2023; 24:813.
<https://doi.org/10.3390/ijms24010813>
PMID:36614254
 23. You X, Wu J, Zhao X, Jiang X, Tao W, Chen Z, Huang C, Zheng T, Shen X. Fibroblastic galectin-1-fostered invasion and metastasis are mediated by TGF- β 1-induced epithelial-mesenchymal transition in gastric cancer. *Aging (Albany NY).* 2021; 13:18464–81.
<https://doi.org/10.18632/aging.203295>
PMID:34260413
 24. Lau LS, Mohammed NBB, Dimitroff CJ. Decoding Strategies to Evade Immunoregulators Galectin-1, -3, and -9 and Their Ligands as Novel Therapeutics in Cancer Immunotherapy. *Int J Mol Sci.* 2022; 23:15554.
<https://doi.org/10.3390/ijms232415554>
PMID:36555198
 25. Kang HG, Kim WJ, Kang HG, Chun KH, Kim SJ. Galectin-3 Interacts with C/EBP β and Upregulates Hyaluronan-Mediated Motility Receptor Expression in Gastric Cancer. *Mol Cancer Res.* 2020; 18:403–13.
<https://doi.org/10.1158/1541-7786.MCR-19-0811>
PMID:31822520
 26. Choi SI, Seo KW, Kook MC, Kim CG, Kim YW, Cho SJ. Prognostic value of tumoral expression of galectin-9 in gastric cancer. *Turk J Gastroenterol.* 2017; 28:166–70.
<https://doi.org/10.5152/tjg.2017.16346>
PMID:28492371
 27. Chong Y, Tang D, Xiong Q, Jiang X, Xu C, Huang Y, Wang J, Zhou H, Shi Y, Wu X, Wang D. Galectin-1 from cancer-associated fibroblasts induces epithelial-mesenchymal transition through β 1 integrin-mediated upregulation of Gli1 in gastric cancer. *J Exp Clin Cancer Res.* 2016; 35:175.
<https://doi.org/10.1186/s13046-016-0449-1>
PMID:27836001
 28. Chen J, Zhou SJ, Zhang Y, Zhang GQ, Zha TZ, Feng YZ, Zhang K. Clinicopathological and prognostic significance of galectin-1 and vascular endothelial growth factor expression in gastric cancer. *World J Gastroenterol.* 2013; 19:2073–9.

- <https://doi.org/10.3748/wjg.v19.i13.2073>
PMID:23599627
29. Sutani T, Sakata T, Nakato R, Masuda K, Ishibashi M, Yamashita D, Suzuki Y, Hirano T, Bando M, Shirahige K. Condensin targets and reduces unwound DNA structures associated with transcription in mitotic chromosome condensation. *Nat Commun.* 2015; 6:7815.
<https://doi.org/10.1038/ncomms8815>
PMID:26204128
30. Fagerberg L, Hallström BM, Oksvold P, Kampf C, Djureinovic D, Odeberg J, Habuka M, Tahmasebpoor S, Danielsson A, Edlund K, Asplund A, Sjöstedt E, Lundberg E, et al. Analysis of the human tissue-specific expression by genome-wide integration of transcriptomics and antibody-based proteomics. *Mol Cell Proteomics.* 2014; 13:397–406.
<https://doi.org/10.1074/mcp.M113.035600>
PMID:24309898
31. Yu H, Zou D, Ni N, Zhang S, Zhang Q, Yang L. Overexpression of NCAPG in ovarian cancer is associated with ovarian cancer proliferation and apoptosis via p38 MAPK signaling pathway. *J Ovarian Res.* 2022; 15:98.
<https://doi.org/10.1186/s13048-022-01030-z>
PMID:35986371
32. Abbaszadegan MR, Taghehchian N, Aarabi A, Nozari S, Saburi E, Moghbeli M. Kindlin1 As a Gender and Location-Specific Diagnostic Marker in Gastric Cancer Patients. *Iran J Pathol.* 2022; 17:23–8.
<https://doi.org/10.30699/IJP.2021.526950.2603>
PMID:35096085
33. Zhang X, Zhu M, Wang H, Song Z, Zhan D, Cao W, Han Y, Jia J. Overexpression of NCAPG inhibits cardia adenocarcinoma apoptosis and promotes epithelial-mesenchymal transition through the Wnt/ β -catenin signaling pathway. *Gene.* 2021; 766:145163.
<https://doi.org/10.1016/j.gene.2020.145163>
PMID:32980450
34. Sun Y, Lin C, Ding Q, Dai Y. Overexpression of FOXC1 Promotes Tumor Metastasis by Activating the Wnt/ β -Catenin Signaling Pathway in Gastric Cancer. *Dig Dis Sci.* 2022; 67:3742–52.
<https://doi.org/10.1007/s10620-021-07226-5>
PMID:34427817
35. Li Y, Liu C, Zhang X, Huang X, Liang S, Xing F, Tian H. CCT5 induces epithelial-mesenchymal transition to promote gastric cancer lymph node metastasis by activating the Wnt/ β -catenin signalling pathway. *Br J Cancer.* 2022; 126:1684–94.
<https://doi.org/10.1038/s41416-022-01747-0>
PMID:35194191
36. Chen J, Wang X, Zhang J, Chang J, Han C, Xu Z, Yu H. Effects of the Wnt/ β -Catenin Signaling Pathway on Proliferation and Apoptosis of Gastric Cancer Cells. *Contrast Media Mol Imaging.* 2022; 2022:5132691.
<https://doi.org/10.1155/2022/5132691>
PMID:36082059
37. Wang Y, Zheng L, Shang W, Yang Z, Li T, Liu F, Shao W, Lv L, Chai L, Qu L, Xu Q, Du J, Liang X, et al. Wnt/ β -catenin signaling confers ferroptosis resistance by targeting GPX4 in gastric cancer. *Cell Death Differ.* 2022; 29:2190–202.
<https://doi.org/10.1038/s41418-022-01008-w>
PMID:35534546